Paleoceanography and Paleoclimatology

RESEARCH ARTICLE
10.1029/2018PA003444

Improving North Atlantic Marine Core Chronologies Using ^{230}Th Normalization

L. Missiaen[1,2], C. Waelbroeck[1], S. Pichat[3,1,4], S. L. Jaccard[5], F. Eynaud[6], R. Greenop[7], and A. Burke[7]

[1]Laboratoire des Sciences du Climat et de l'Environnement, LSCE/IPSL, CEA-CNRS-UVSQ-Université Paris Saclay, Gif-sur-Yvette, France, [2]Climate Change Research Centre, University of New South Wales, Sydney, New South Wales, Australia, [3]Université de Lyon, ENS de Lyon, Laboratoire de Géologie de Lyon (LGL-TPE), Lyon, France, [4]Climate Geochemistry Department, Max Planck Institute for Chemistry, Mainz, Germany, [5]Institute of Geological Sciences and Oeschger Center for Climate Change Research, University of Bern, Bern, Switzerland, [6]Université de Bordeaux, UMR EPOC 5805, Pessac, France, [7]School of Earth and Environmental Science, Irvine Building, University of St Andrews, St Andrews, United Kingdom

Key Points:
- We evaluated Th normalization as a means to refine the age models for three North Atlantic cores
- The revised chronologies imply that the cooling at the onset of Heinrich Stadial 1 was synchronous with an increase in the Greenland Ca^{2}
- Greenland ice Ca^{2+} rise at 17.48 ± 0.21 ka can serve as a new tie point for the transition into Heinrich Stadial 1 in North-Atlantic cores

Supporting Information:
- Supporting Information S1
- Data Set S1

Correspondence to:
L. Missiaen,
l.missiaen@unsw.edu.au

Citation:
Missiaen, L., Waelbroeck, C., Pichat, S., Jaccard, S. L., Eynaud, F., Greenop, R., & Burke, A. (2019). Improving North Atlantic marine core chronologies using ^{230}Th normalization. *Paleoceanography and Paleoclimatology*, *34*. https://doi.org/10.1029/2018PA003444

Received 20 JUL 2018
Accepted 24 MAY 2019
Accepted article online 3 JUN 2019

Abstract Producing independent and accurate chronologies for marine sediments is a prerequisite to understand the sequence of millennial-scale events and reveal potential temporal offsets between marine and continental records, or between different marine records, possibly from different regions. The last 40 ky is a generally well-constrained period since radiocarbon (^{14}C) can be used as an absolute dating tool. However, in the northern North Atlantic, calendar ages cannot be directly derived from ^{14}C ages, due to temporal and spatial variations of surface reservoir ages. Alternatively, chronologies can be derived by aligning Greenland ice-core time series with marine surface records. Yet this approach suffers from the lack of clearly defined climatic events between 14.7 and 23.3 cal ky BP (hereafter ka), a crucial period encompassing Heinrich Stadial 1 and the onset of the last deglaciation. In this study, (i) we assess the benefits of ^{230}Th normalization to refine the sedimentation history between surface temperature alignment tie points and (ii) revisit the chronologies of three North Atlantic marine records. Our study supports the contention that the marked increase in the Greenland Ca^{2+} record at 17.48 ka ± 0.21 ky (1σ) occurred within dating uncertainty of sea surface temperature cooling in the North Atlantic at the onset of Heinrich Stadial 1. This sharp feature might be useful for future chronostratigraphic alignments to remedy the lack of chronological constraint between 14.7 and 23.3 ka for North Atlantic marine records that are subject to large changes in ^{14}C surface reservoir age.

1. Introduction

Greenland ice core records have revealed abrupt climate variability during most of the last glacial cycle. Several mechanisms have been proposed to explain the origin of these abrupt climate changes, some of which involve planetary waves, sea ice, ice-sheet dynamics, or low to high latitude teleconnections (see Clement & Peterson, 2008, for a review). However, the prevailing paradigm relates these abrupt climatic events to changes in the Atlantic Meridional Overturning Circulation (Böhm et al., 2015; Henry et al., 2016; Lynch-Stieglitz, 2017; Rahmstorf, 2002). Thus, the study of water mass reorganizations and circulation changes across those abrupt climate events remains central for a better understanding of the underlying physical mechanisms. As those events only last for a few centuries up to a few millennia, producing independent and accurate chronologies for marine archives is a key aspect, especially when assessing temporal lead/lag relationships between marine and continental records or between different marine records, possibly from different regions.

To date, several methods have been applied to establish marine record chronologies. The last 40 ky is a particularly well-dated period because it corresponds to the approximate time range covered by radiocarbon dating, enabling the construction of accurate marine core chronologies through ^{14}C dating of (preferably single species) planktonic foraminifera samples. Raw radiocarbon ages are converted into calendar ages using calibration curves (e.g., IntCal13; Reimer et al., 2013). A downcore age model is then derived from these dated levels, using more or less sophisticated methods. The simplest approach assumes a constant sedimentation rate between the dated levels, whereas software based on Bayesian methods (e.g., OxCal (Ramsey, 2009), Bchron (Parnell et al., 2008), Bacon (Blaauw, 2010), and Undatable (Lougheed & Obrochta, 2019))

produce more sophisticated age-depth relationships by including additional stratigraphic information and providing age uncertainties of the dated levels using a Monte Carlo approach. The latest improvements even take into account the uncertainty of the sampling depth (Lougheed & Obrochta, 2019). Additionally, those tools also provide the opportunity to statistically test the consistency of the ^{14}C dates and generate realistic age uncertainties that increase with the distance from the dated depth horizons, making them, at present, the best option to build robust age models.

Despite the development of sophisticated age-depth models in recent decades, there is growing evidence for further complications affecting the use of ^{14}C to robustly date marine sediments. For instance, different planktonic foraminifer species from the same sediment depth level may have significantly different radiocarbon ages in reworked sediments or in samples that have undergone recrystallization and incorporation of secondary radiocarbon (Broecker et al., 2006). It has also been shown that bioturbation, carbonate dissolution, or chemical erosion could significantly influence radiocarbon-based age scales (Bard, Arnold, Duprat, et al., 1987; Barker et al., 2007; Mekik, 2014; Wycech et al., 2016). Therefore, special care has to be taken when measuring radiocarbon in locations where the sediment accumulation rate is low and where there is evidence of intense bioturbation or secondary calcite crystallization. Last but not least, converting marine radiocarbon dates into calendar ages requires knowledge about the ^{14}C age difference between the ocean surface waters and the contemporary atmosphere, commonly referred as the surface reservoir age. This surface reservoir age is quite well constrained in the modern ocean (see Key et al., 2004), but as it depends on the kinetics of air-sea gas exchange and on the location of deep-water formation, it can vary both spatially and temporally. In particular, it has been shown that north of ~40°N in the Atlantic, surface reservoir ages have undergone large variations through time due to changes in sea ice cover or deep-water formation (Bard et al., 1994; Bondevik et al., 2006; Thornalley et al., 2011; Waelbroeck et al., 2001). To date, surface reservoir age variations remain poorly constrained; therefore, simply relying on ^{14}C to build accurate chronologies for North Atlantic marine records, especially for those located north of ~40°N, is problematic.

When dating northern North Atlantic cores over the last 40 ky, a classical approach consists of assuming that abrupt changes in sea surface temperature (SST) are synchronous with rapid air temperature variations in Greenland (e.g., Austin & Hibbert, 2012). This is equivalent to assuming that the equilibration time between air temperature and surface water temperature is short enough to be neglected, which appears reasonable when considering the currently achievable precision in marine sediment chronologies (a few hundred years at best). This method has been, and still is, very valuable for North Atlantic sites, especially north of ~40°N where calendar ages cannot reliably be derived from ^{14}C dates due to poorly constrained variations in surface reservoir ages. However, the age models derived by aligning SST to Greenland air temperature suffer from the lack of well-defined, high-amplitude climatic events in the Greenland temperature (or ice $\delta^{18}O$) records in the interval from 27.73 to 14.64 ka in the GICC05 age scale (Wolff et al., 2010). During this 13 ky long interval, there is only one small abrupt warming dated at 23.29 ka $\pm$ 0.4 ky (Wolff et al., 2010), which might be difficult to identify in marine SST records. Consequently, North Atlantic marine records, located in the vicinity of deep-water formation areas and thus in key regions for studying ocean circulation changes, are particularly difficult to precisely date over this time interval, which includes the last two Heinrich events and the Last Glacial Maximum. Thus, improving constraints on marine chronologies for this time period (0–30 ka) will help to better constrain the timing of oceanic changes leading to Heinrich events and the last deglaciation.

Sedimentary ^{230}Th excess ($^{230}Th_{xs}$) has been widely used to reconstruct past changes in the vertial particle flux (see François et al., 2004, for a review). However, in cases where the sediment lateral redistribution (i.e., focusing or winnowing) can be either assumed to be constant across the study interval (Bourne, Thomas, et al., 2012) or independently estimated (Adkins et al., 1997), ^{230}Th normalization can also be used as a tool to refine marine core sedimentation rate history between independently dated levels. The sedimentation rate inferred from two consecutive dated levels (i.e., either calibrated ^{14}C ages or tie point alignment) is variably adjusted using changes in $^{230}Th_{xs}$, corrected for radioactive decay since deposition (subscript "0"), $^{230}Th_{xs,0}$ (see section 2.2 for detailed method description). $^{230}Th_{xs,0}$ data can be produced at high resolution through intervals with a limited number of tie points, potentially improving marine core chronologies across these time periods. To date, despite its apparent advantages, the use of Th normalization to refine marine cores age models has been relatively limited (Adkins et al., 1997; Bourne, Mac Niocaill, et al., 2012).

Table 1
Records Used in This Study

Core	Lat (°N)	Lon	Depth (m)	^{14}C data	Radioisotope data (^{230}Th, ^{232}Th, ^{238}U)	Foraminifer-based SST
SU90-08	43.05	30.03°W	3080	Missiaen et al. (2018), Vidal et al. (1997)	Missiaen et al. (2018)	Missiaen et al. (2018); *full data set in supporting material*
SU90-03	40.05	32°W	2475	Chapman et al. (2000)	This study	Cortijo et al. (1999)
SU81-18	37.76	10.18°W	3135	Bard, Arnold, Maurice, et al. (1987), Waelbroeck et al. (2001)	Gherardi et al. (2005, 2009)	Bard, Arnold, Maurice, et al. (1987), Waelbroeck et al. (2001)
MD03-2705	18.1	21.2°E	3085	Jullien et al. (2007), Matsuzaki et al. (2011)	Meckler et al. (2013)	Matsuzaki et al. (2011)

Note. SST = sea surface temperature.

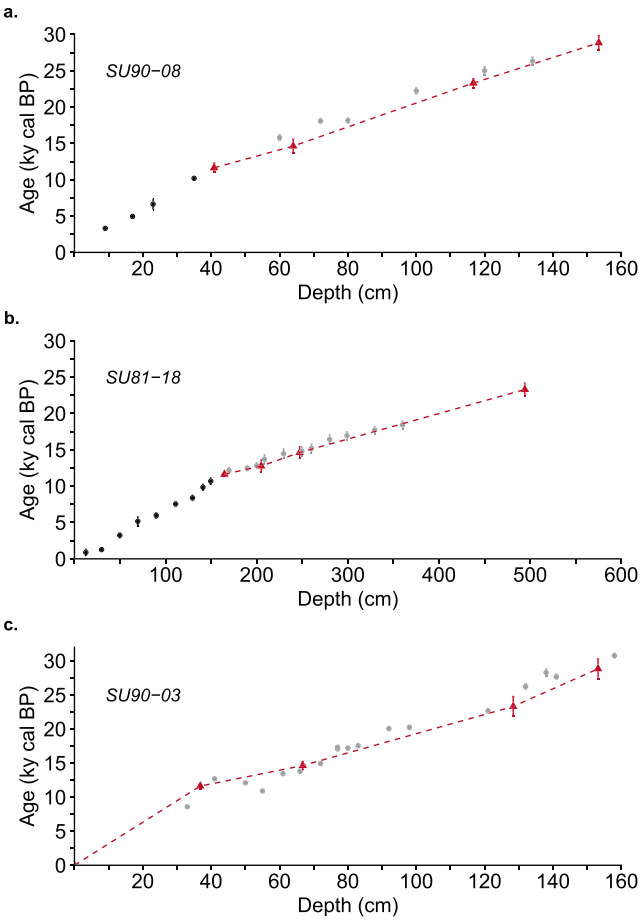

Figure 1. Evaluation of the sea surface temperature (SST) alignment tie points for SU90-08, SU81-18, and SU90-03. The red triangles represent the alignment tie points (SST vs. NGRIP δ^{18}O) with 2σ uncertainty. The red dashed line corresponds to the linear interpolation between the SST alignment tie points. The dots represent the calibrated ^{14}C ages assuming a constant surface reservoir age (see text) with 2σ uncertainty. The black dots were used to constrain the Holocene age-depth relationships, and the grey dots were not used for age model construction because of likely surface reservoir age variations. The upper 80 cm of SU90-03 displays radiocarbon age reversals and inconsistencies between radiocarbon and alignment stratigraphic information (see Figure S2). We thus chose to consider only the SST alignment tie points in the final age model.

In this study we investigate the potential benefits of the Th normalization method to determine robust age models for northern North Atlantic (north of ~40°N) marine sediment cores over the last 25 ky. First, we discuss the assumptions underlying the Th normalization approach. Second, we evaluate the consistency of sedimentation rate changes inferred from Th normalization and radiocarbon dating for a core retrieved from the tropical Atlantic, which has likely not undergone large variations in surface reservoir ages. Finally, we propose new age models based on the integration of surface record alignments and Th normalization for three North-Atlantic records and evaluate the implications for their SST records.

2. Material and Methods

2.1. Core Locations and Available Data

Our study requires the following data to be available: high-resolution downcore SST reconstructions to allow accurate alignment with ice core records and high-resolution ^{238}U, ^{230}Th, and ^{232}Th activities between dated levels. Such a combination of data was available in only a few locations. Among those, we selected low latitude core MD03-2705 and North-Atlantic cores SU81-18, SU90-03, and SU90-08 (Table 1, Table S1, and Figure S1 in the supporting information) because they had high-resolution $^{230}Th_{xs,0}$ records. All selected records cover the last deglaciation and the interval of particular interest from 14.64 to 23.29 ka for which no alignment tie point can be defined in Greenland ice δ^{18}O record.

Core MD03-2705 is located in the tropical Atlantic, far from fluctuating sea ice cover and deep-water formation areas and away from coastal upwelling. Thus, at this location, surface reservoir age is assumed to have remained close to the modern value of 470 ± 120 years (GLODAP (Key et al., 2004)) throughout the studied period. This core is thus particularly well suited for a comparison of the sedimentation rate history obtained from radiocarbon and Th-normalization approaches (see section 4.1.3).

Cores SU90-08, SU90-03, and SU81-18 are well-studied reference cores with numerous paleoproxy records and thus good candidates to test the potential of the Th-normalization technique to produce improved age-depth models. Among these three cores, SU90-08, located in the Ice Rafted Detritus (IRD) belt, exhibits remarkably high amplitude $^{230}Th_{xs,0}$ changes (Missiaen et al., 2018), making this core a candidate for substantial age-model change with Th normalization. For these cores (which are either close or north of 40°N), we only use the published radiocarbon

dates younger than 10 ka as chronological markers because the surface reservoir ages are likely to have significantly varied before the Holocene (see Text S1, Figure S2, and Tables S2 to S5). To constrain the older part of the age-depth relationships, we establish a set of tie points based on the alignment of the SST records to NorthGreenland Ice-core Project (NGRIP) ice $\delta^{18}O$ (Andersen et al., 2006; Rasmussen et al., 2006; Svensson et al., 2006; Vinther et al., 2006) using the AnalySeries software (Paillard et al., 1996) and assuming synchronicity of rapid warming in both archives during the events defined by Wolff et al. (2010); see Tables S6 to S8). We verified the SST alignment tie points using radiocarbon dates. To do so, we converted the published raw radiocarbon ages into calendar ages using Oxcal (online version 4.3; Ramsey, 2009), the IntCal13 calibration curve (Reimer et al., 2013), and the modern reservoir age corresponding to each location extracted from GLODAP (Key et al., 2004; 400 ± 100 years for SU90-08 and SU90-03, respectively, and 500 ± 100 years for SU81-18). We then verified that for a given depth level, the assigned calendar age (derived from the alignment age model) was either younger or within error of the calendar age derived from ^{14}C measurements assuming that the reservoir age has been constant and identical to the modern value at the considered location (see Figure 1). In other words, we ensure that the reservoir ages implied by our Greenland tie points in the pre-Holocene northern North Atlantic are not younger than modern.

Figure 2 compares the age-depth relationships derived by the two methods: (i) assuming constant sedimentation rate between tie points and (ii) using the $^{230}Th_{xs,0}$ measurements to compute sedimentation rate changes between tie points. The latter method requires a set of assumptions that are described in the following section.

2.2. Th Normalization as a Dating Tool

The Th-normalization technique requires the determination of the "excess" ^{230}Th activity in the sediments derived from the scavenging of ^{230}Th from the water column by sinking particles (i.e., ^{230}Th that is not incorporated within the mineral lattice or supported by radioactive decay from authigenic uranium) and corrected for radioactive ^{230}Th decay since sediment deposition (termed excess thorium [$^{230}Th_{xs,0}$]). The underlying assumptions are discussed in detail in section 4.1.1. The equations used to determine the ^{230}Th excess activities ($^{230}Th_{xs}$) are the following (Henderson & Anderson, 2003):

$$^{230}Th_{xs} = {}^{230}Th_{meas} - {}^{230}Th_{det} - {}^{230}Th_{auth} \quad (1)$$

where "meas" stands for the measured activity in the bulk sediments and "det" and "auth" are for the detrital and authigenic fractions, respectively.

Equation (1) can be rewritten as follows:

$$\begin{aligned} {}^{230}Th_{xs} = {}^{230}Th_{meas} &- \left({}^{232}Th_{meas} \times (U/Th)_{det}\right) \\ &- \left[\left({}^{238}U_{meas} - \left({}^{232}Th_{meas} \times (U/Th)_{det}\right)\right) \right. \\ &\times \left\{\left(1 - e^{-\lambda_{230} t}\right) + \frac{\lambda_{230}}{\lambda_{230} - \lambda_{234}} \left(\left(\frac{^{234}U}{^{238}U}\right)_{sw}\right) - 1\left(e^{-\lambda_{234} t}\right) \right. \\ &\left. \left. - e^{-\lambda_{230} t}\right\}\right] \end{aligned} \quad (2)$$

where λ_x is the decay constant of the considered isotope and t is the calendar age of the sediments. ($^{234}U/^{238}U$) ratio is assumed to be that of sea water: $(^{234}U/^{238}U)_{sw} = 1.1467$ ($1\sigma = 0.0025$; Robinson et al., 2004), $(U/Th)_{det}$ is the ($^{238}U/^{232}Th$) activity ratio of the sediment detrital fraction the latter being considered as either constant or variable with time (see Missiaen et al., 2018).

Finally, the excess fraction at the time of sediment deposition $^{230}Th_{xs,0}$ can be calculated by correcting $^{230}Th_{xs}$ for the radioactive decay:

$$Th_{xs,0} = Th_{xs}\, e^{\lambda_{230} t} \quad (3)$$

As proposed by Adkins et al. (1997) and further developed by Bourne, Thomas, et al. (2012), Bourne, Mac Niocaill, et al. (2012), $^{230}Th_{xs,0}$ can be used to refine age models by constraining the sedimentation rate inferred between two dated levels. ^{230}Th is produced by the decay of dissolved ^{234}U in the water column,

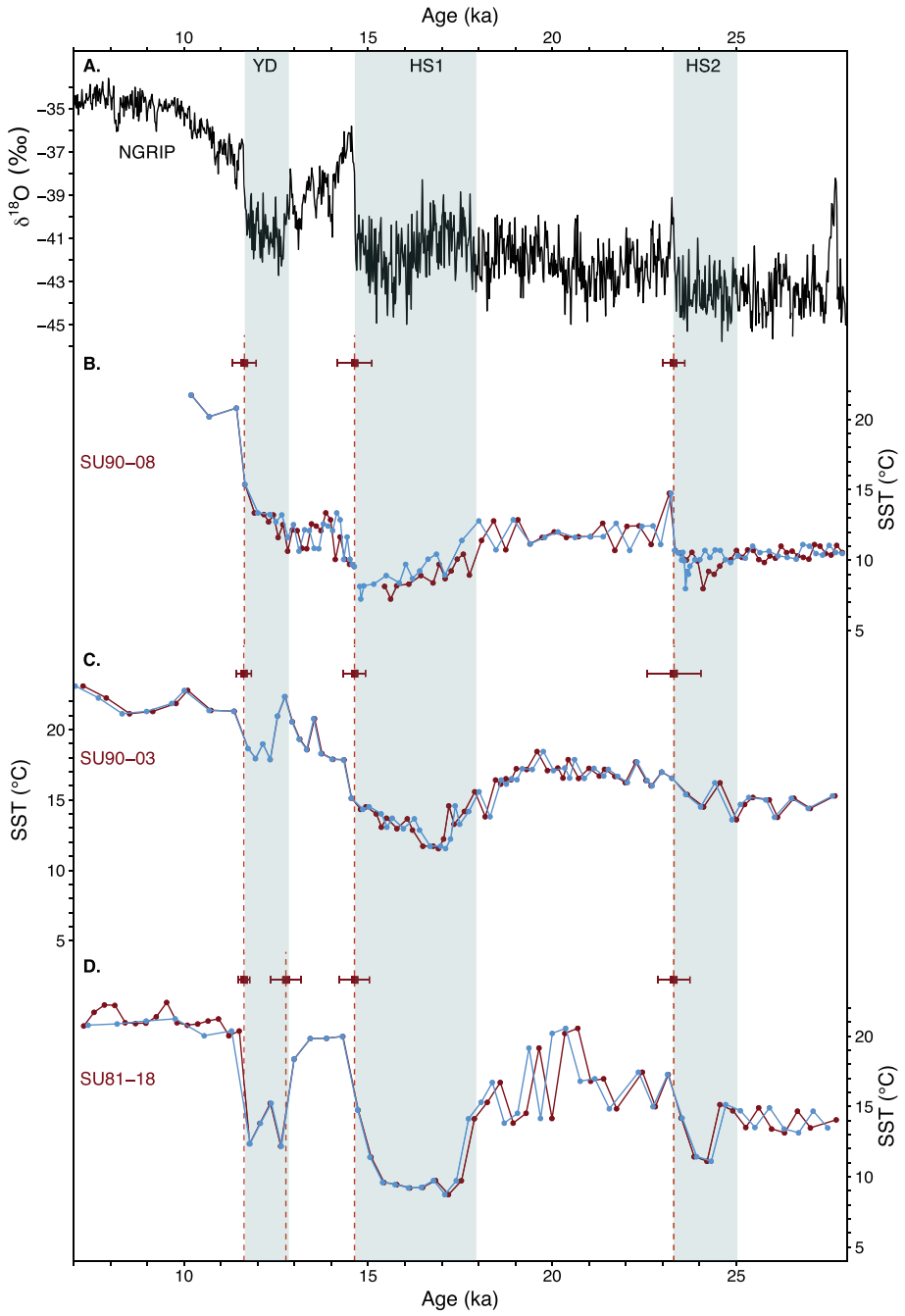

Figure 2. Impact of Th normalization on the chronologies for sea surface temperature (SST) reconstructions. (a) $\delta^{18}O$ of the ice at NGRIP (Andersen et al., 2006; Rasmussen et al., 2006; Svensson et al., 2006; Vinther et al., 2006) and SST records (see Table 1) of core SU90-08 (b), SU90-03 (c), and SU81-18 (d). For each subplot, the red squares represent the SST alignment tie points and corresponding 1σ uncertainty (Tables S6 to S8), the red curve age scale is based on the SST alignment tie points, and the blue curve age scale is based on Th normalization between dated levels. Grey bands represent the Younger Dryas and Heinrich Stadial 1 and 2 chronozones.

where it is rapidly scavenged onto the surface of sinking particles. As ^{230}Th has a very short residence time in the water column (ranging from a few months in surface waters up to 50 years in deep waters; François, 2007), all of the ^{230}Th produced in the water column is rapidly removed to the underlying sediments via particle scavenging. At a given location, the amount of ^{230}Th produced in the water column is constant through time and is controlled by the water depth. If all of the ^{230}Th produced in the water column

reaches the underlying sediments, the activity of $^{230}Th_{xs,0}$ in the sediment is dependent on sediment supply and thus sedimentation rate variations. In this case, the $^{230}Th_{xs,0}$ should be inversely proportional to the sedimentation rate. Sedimentation rate increases are inferred from relative decrease of $^{230}Th_{xs,0}$, reflecting an effective dilution of the ^{230}Th. Conversely, increases of $^{230}Th_{xs,0}$ are interpreted as a reduction in the sedimentation rate. $^{230}Th_{xs,0}$ can then be used to correct the average sedimentation rate inferred from available dated levels, using the following expression (Bourne, Thomas, et al., 2012):

$$S_i = S_a \frac{Th_{mean}}{Th_i} \quad (4)$$

where S_i is the corrected sedimentation rate for interval i ($i = 1$ to n intervals between two bracketing dated levels), S_a and Th_{mean} are the average linear sedimentation rate and weighted average of $^{230}Th_{xs,0}$ between two bracketing dated levels, respectively, and Th_i is the $^{230}Th_{xs,0}$ of interval i. Importantly, this method assumes that the sediment lateral redistribution remains constant throughout the interval of time between the bracketing dated levels and so may not be applicable to cores with large temporal variations in their sedimentary regimes. However, for cores with minimal variations of lateral redistribution relative to changes in vertical sediment accumulation, this method provides a means to reconstruct sedimentation rate variations at a higher-resolution than what can be achieved using only the dated levels.

In this study, we revisit the chronologies of North Atlantic cores SU81-18, SU90-03, and SU90-08 using both the published and newly generated data listed in Table 1. After aligning the SST estimates to the NGRIP $\delta^{18}O_{ice}$ record, we used the Th-normalization approach outlined above. From the SST alignment tie points, we first derive an age model by linear interpolation and calculate the downcore evolution of $^{230}Th_{xs,0}$ (equations (2) and (3)). Then, using equation (4), we compute a corrected sedimentation rate history and derive a revised age model. As $^{230}Th_{xs,0}$ is age-model dependent, we iterate the process 20 times, that is, until a stable age model was reached.

2.3. ^{230}Th Measurements

^{230}Th for core SU90-03 was measured by isotopic dilution using a ^{229}Th spike on a single collector, sector field inductively coupled plasma mass spectrometry at the University of British Columbia following the procedure described by Choi et al. (2001); see Table S1). In short, the samples were first acidified with HCl, spiked with ^{229}Th, and equilibrated for 24 hr. Then, the samples were fully digested with an HNO_3-HF mixture. The Fe-oxy-hydroxides, which adsorb or entrain dissolved and particulate Th, were precipitated by adjusting the pH to 8–9 and isolated by centrifugation. After dissolving the residue, the Th fraction was extracted and then purified using two anion exchange columns (AG1-X8 resin). The Th fraction was filtered prior to its measurement.

3. Results: Impact of Th Normalization on Marine Core Chronologies

The magnitude of the age model change due to Th normalization is very different depending on the core location (Figure 2). Among the cores under investigation, the inferred age changes range from less than a year to 940 years. More specifically, for cores SU81-18 and SU90-03, there are negligible changes when comparing the simple linear interpolation between dated levels and the Th-normalized age model, with, on average, age differences of less than 100 years. However, some parts of the records are characterized by larger discrepancies, 120–300 years between 17.4 and 21 ka for SU81-18 and around 150 years between 15 and 21 ka for SU90-03. The alignment dating uncertainty mainly arises from the difficulty in identifying common temperature trends in the marine and Greenland ice records as well from the uncertainties in dating the Greenland reference record itself (Wolff et al., 2010). For SU81-18, the (1σ) uncertainty increases from 150 years around the Younger Dryas (12.7–11.7 ka) to 440 years around 23 ka. For SU90-03, the (1σ) uncertainty is generally higher (mainly because the SST transitions are less well defined) and increases from 206 years around the YD to 700 years around 23 ka. Thus, for these two cores, the age model changes due to Th normalization remain smaller than the uncertainty on the dated levels themselves. For the interval between 23.29 and 14.64 ka, the age change due to Th normalization corresponds to about half of the dated levels uncertainty for SU90-03 and up to three-quarter of the dated levels uncertainty for SU81-18.

SU90-08 displays the largest chronological disparities, with an average age difference of about 450 years. The largest discrepancy is observed around 16.5 ka and corresponds to an age change of about 940 years. For comparison, the uncertainty on the alignment-dated levels is smaller than 400 years before 23.29 ka (Table S6). Thus, Th normalization has a significant impact on the SU90-08 age model, especially across Heinrich layers that are characterized by the largest $^{230}Th_{xs,0}$ variations (Figure S6). During these intervals, the ^{230}Th-corrected sedimentation rate is up to 4–5 times larger than the background sedimentation rate (Figure S6). In the case of SU90-08, the high variability in the $^{230}Th_{xs,0}$ record results in a drastic increase in sedimentation rate during the Heinrich events. This is indeed expected because additional detrital material would have been transported to the core site by drifting icebergs during these events.

4. Discussion

4.1. Th-Normalization Validation

The use of radiogenic Th isotopes to reconstruct past sediment fluxes has first been proposed by (Bacon & Rosholt, 1982) and widely used since then (e.g., Suman & Bacon, 1989, and see François et al., 2004, for a review). Because ^{230}Th has been found to be sensitive to changes in particle size or type (e.g., Chase et al., 2002), or because of necessary reconsiderations of the $^{230}Th_{xs,0}$ calculation method (e.g., Bourne, Thomas, et al., 2012; Missiaen et al., 2018), the use of Th normalization to reconstruct sedimentary fluxes has remained a matter of debate (Broecker, 2008; Marcantonio et al., 2014). However, modeling work (Henderson et al., 1999), sediment trap (Yu et al., 2001) and marine core data (Costa & McManus, 2017) indicate that Th normalization can be used to accurately reconstruct past variations in sediment accumulation.

In this study, we use Th normalization to refine the sedimentation rate history between dated levels, an approach that has yet only been rarely applied (e.g., Adkins et al., 1997; Bourne, Mac Niocaill, et al., 2012). Because of the specific use of $^{230}Th_{xs,0}$ and because our study deals with high-precision dating, it is worthwhile to summarize the underlying assumptions of the method first.

4.1.1. Underlying Assumptions of the Th-Normalization Method

As highlighted in Bourne, Thomas, et al. (2012), the Th-normalization method relies on the following six assumptions:

1. Lateral transport of ^{230}Th in the water column is negligible. This assumption is likely valid for the cores studied here given the high particle-reactivity of ^{230}Th and thus its short residence time in the water column (from a few months up to 50 years for sluggishly ventilated deep waters; François, 2007) compared to the deep ocean circulation rates.
2. The ^{232}Th content of the sediment is assumed to be entirely of detrital origin, and the lithogenic material is in secular equilibrium, that is, $(^{238}U)_{det} = (^{230}Th)_{det.}$. This hypothesis is discussed in detail in Bourne, Thomas, et al. (2012).
3. The incorporation of authigenic uranium occurs at the time of sediment deposition at a known and constant $(^{234}U/^{238}U)$ ratio, generally assumed to be that of seawater, $(^{234}U/^{238}U)_{sw} = 1.1467$ ($1\sigma = 0.0025$; Robinson et al., 2004).

A better assessment of the initial $(^{234}U/^{238}U)$ can be obtained with ^{234}U data, but ^{234}U data have rarely been published along with the Th data. In the absence of evidence for a higher initial $(^{234}U/^{238}U)$, we use the seawater value in this study.

The estimation of the $^{230}Th_{auth}$ also assumes that the U content has been preserved since the sediment deposition. Indeed, changes in the bottom water oxygenation could lead to a substantial decrease of the authigenic U content by postdepositional dissolution processes sometimes referred as "burndown" (see (Jacobel et al., 2017)). In such cases, the method presented here would underestimate the $^{230}Th_{auth}$ and thus overestimate the $^{230}Th_{xs,0}$, especially for old sediments. However, postdepositional dissolution of authigenic U is unlikely to produce significant biases in the $^{230}Th_{xs,0}$ in the studied cores over the last 25 ky because (i) $^{230}Th_{auth}$ represents at most 10% of the total ^{230}Th measured in these cores (see Missiaen et al., 2018) and (ii) the potential ingrowth of authigenic ^{230}Th from ^{234}U (half-life 245 ky) would not be substantial over the last 25 ky.

4. A well-constrained age model is established by accurately defined dated levels. Indeed, as explained in section 2.2, the method does not alter the age of the dated levels but refines the sedimentation rate and

age model in between. The dated levels used in this study are shown in Figure 1 (see supporting information for further details).

5. The value of $(U/Th)_{det}$, which represents the ($^{238}U/^{232}Th$) activity ratio of the detrital fraction, and its temporal evolution are sufficiently constrained (Missiaen et al., 2018). This assumption is discussed in further detail in section 4.1.2.
6. Sediment focusing is constant between tie points.

This last assumption mainly implies that the sedimentary environment would have remained broadly stable through time. In other words, the changes in material inputs to the core location due to lateral sediment redistribution (i.e., focusing or winnowing) would be limited compared to vertical sediment flux.

Assessing changes in lateral sediment redistribution through time is however not straightforward. Bourne, Thomas, et al. (2012) proposed either (i) to check the sediment composition to track potential changes in sediment type or (ii) to carry out sortable silt and magnetic properties measurements to retrieve independent constraints on sediment transport by deep currents and grain size variability. However, none of these measurements is a direct indicator of lateral sediment redistribution. Indeed, changes in those sediment properties such as composition or grain size can also be due to changes in vertical inputs, related either to changes in biologic productivity or to dust supply.

The lateral sediment redistribution can also be assessed using the ^{230}Th data itself by calculating the focusing factor ψ (see Text S2 for detailed explanation and François et al., 2004, for a review). First, in order to compute sediment focusing, it is necessary to assess the downcore evolution of the dry bulk density, a measurement that is not routinely done on marine sediment cores and that is not available for the cores studied here. In the absence of dry bulk density measurements, the latter can be derived from $\%CaCO_3$ (Froelich et al., 1991). Second, the focusing factor ψ can only be calculated as an average between well-dated levels and is typically a low-resolution variable. Last, the focusing factor absolute value depends on the accuracy of the age model (Kienast et al., 2007). Adkins et al. (1997) proposed to use the $\%CaCO_3$ as a proxy for sediment focusing. Assuming a constant (in time) linear relation between ψ and $\%CaCO_3$, they calculated a Th-normalized age using the proxy-derived focusing variations. This approach was not applicable to the cores studied here because (i) reliable Holocene radiocarbon dates are needed to constrain the slope between ψ and $\%CaCO_3$ (not applicable for SU90-03; see supporting information) and (ii) this method assumes that the sedimentary regime of the studied time interval is comparable to the one of the Holocene, which is likely not true for the sediment cores studied here due to the presence of IRD layers.

Instead, in order to highlight potential lateral sediment redistribution variations between tie points, we have evaluated the focusing factor for all four cores (see supporting information Text S2). We have calculated the focusing factor ψ on two sets of intervals defined by levels located in between the age-model tie-points (Figure 3). In general, the focusing factor varies between 0.15 and 2, which may reflect changes in sedimentary regime. However, the observed ψ range is much smaller than the values reported in areas characterized by strong sediment redistribution on the seafloor (e.g., $1 < \psi < 4$; Marcantonio et al., 2001). More importantly, for sediment cores SU90-03, SU90-08, and SU81-18, the focusing factor remained broadly constant between 14.7 to 23.3 ka, irrespective of the intervals on which the calculation was performed (Figure 3), accounting for an absence of significant sediment lateral redistribution during this time period. The case of sediment core MD03-2705 is further discussed in section 4.1.3.

Furthermore, based on the analysis of a compilation of magnetic properties measurements for two of the cores studied here (SU81-18, at the same location as MD95-2042 and SU90-08), Kissel (2005) concluded that the only significant changes in magnetic properties were associated with the Heinrich events. The increases in both grain size and relative concentrations of magnetic grains mostly result from lithogenic particle supply from drifting icebergs (Kissel, 2005). Thus, magnetic properties also suggest that in these cores, changes in sedimentary regime were related to changes in the vertical flux of magnetic grains, rather than lateral sediment redistribution.

Importantly, although it seems that the nearly constant sediment focusing is a valid assumption in the case of our three North-Atlantic sediment cores (SU90-08, SU90-03, and SU81-18), in other locations this assumption can be more problematic. Indeed, dramatic changes in bottom currents across abrupt climate events

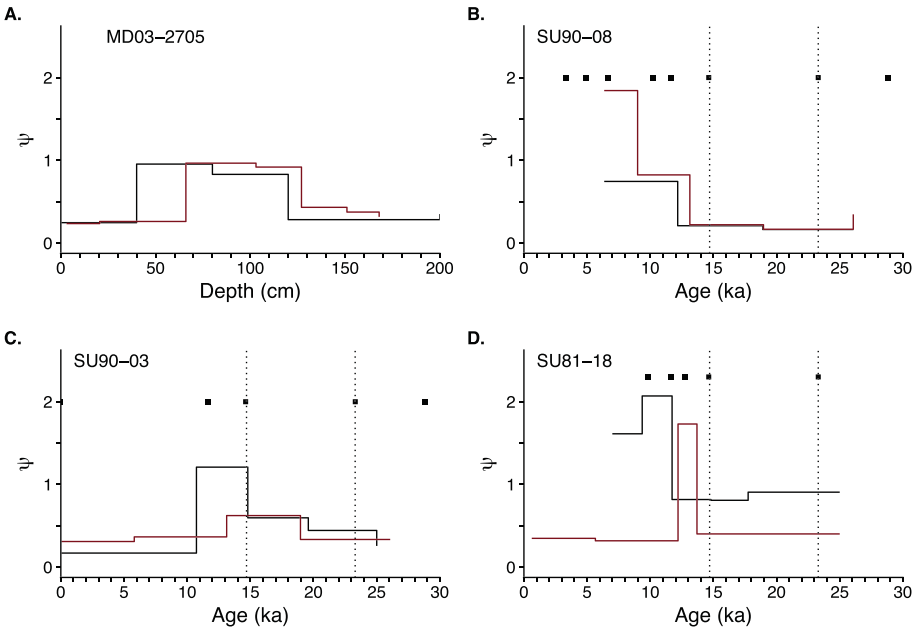

Figure 3. Focusing factor (ψ) calculations. (a) MD03-2705, (b) SU90-08, (c) SU90-03, and (d) SU81-18. MD03-2705 results are plotted against depth as in Figure 5. SU90-03, SU90-08, and SU81-18 results are plotted against age as in Figure 6. The different colors represent the different focusing factor values obtained with different choices of dated levels. As we aim at obtaining information about the focusing factor changes between the dated levels, we calculated it on independent intervals, with the number of intervals being similar to the number of intervals defined by the actual dated levels. The black squares represent the actual tie points, and the vertical dashed lines delimit the interval of interest between 14.7 and 23.3 ka.

have been recorded in the Atlantic (e.g., Hall et al., 2011). In these cases, significant changes in sediment focusing are likely to occur. A careful and case-by-case evaluation of the sediment focusing is a necessary prerequisite to using Th normalization as a way to refine the sedimentation history between independently dated levels.

4.1.2. The Impact of Temporal Variations of the Detrital Material ($^{238}U/^{232}Th$) Ratio

Missiaen et al. (2018) showed that the detrital material ($^{238}U/^{232}Th$) ratio ($(U/Th)_{det}$ hereafter) could vary through time, which significantly affects $^{230}Th_{xs,0}$ records for cores with important detrital input, such as cores from the Iberian margin (SU81-18) or cores located in the IRD belt (SU90-08). Thus, before using Th normalization to refine sediment core age models, we have assessed the impact of a variable $(U/Th)_{det}$ value. We tested this effect using the data set from core SU90-08, particularly well suited for two major reasons. First, to date, SU90-08 is the only core for which $(U/Th)_{det}$ has been measured downcore; it is thus possible to compare age models obtained with the measured $(U/Th)_{det}$ value and with prescribed $(U/Th)_{det}$ values. Second, this core displays high ^{230}Th-normalized flux variations associated with the Heinrich events, which may imply significant sedimentation rate correction and thus age changes when applying the Th-normalization approach. We computed the age models keeping the same dated levels (described in Table S6) with the following $(U/Th)_{det}$ values: constant $(U/Th)_{det}$ of 0.4 or 0.8 or variable $(U/Th)_{det}$ using the values measured by Missiaen et al. (2018).

Changes in the $(U/Th)_{det}$ value have a large effect on the SU90-08 $^{230}Th_{xs,0}$ record, particularly in the Heinrich layers. Missiaen et al. (2018) showed that in the Heinrich layers, the ^{230}Th-normalized flux was multiplied by 2 to 3 in response to a change in $(U/Th)_{det}$ from 0.4 to 0.8. As a result, in response to a 0.4 to 0.8 increase in $(U/Th)_{det}$, we observe a 10% change on average of the sedimentation rate obtained from Th normalization. In the Heinrich layers, the sedimentation rates derived from Th-normalization approach can double depending on the chosen $(U/Th)_{det}$ value (Figure 4). However, changes in the $(U/Th)_{det}$ value do not change the $^{230}Th_{xs,0}$ pattern, which exhibits strong increases in sedimentary flux during Heinrich events. Thus, even with the large changes in sedimentation rate, changes in $(U/Th)_{det}$ value do not produce substantial changes in the Th-normalized age model for sediment core SU90-08 (Figure 4). Extreme

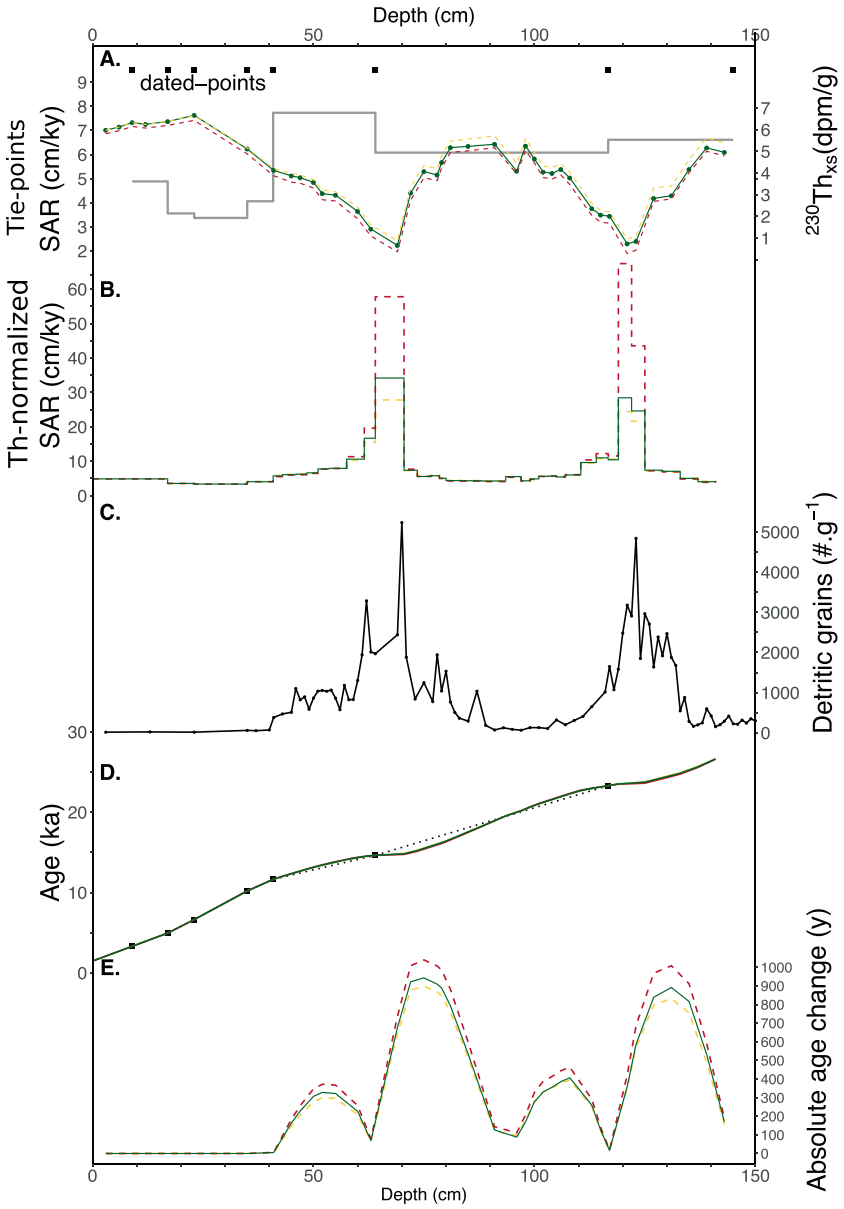

Figure 4. Impact of changes in $(U/Th)_{det}$ on the Th normalization based chronology for SU90-08. (a) Dated levels (black squares), sedimentation rate derived from the dated levels (grey line) and $^{230}Th_{xs,0}$ record. (b) Corrected sedimentation rate after applying Th normalization. (c) Ice Rafted Detritus record showing H1 and H2 detrital peaks. (D) Th-normalization-based age model. The dotted line represents the simple age model derived from linear interpolation between dated levels. (e) Absolute change in age due to Th normalization with respect to the initial chronology based on dated levels. For every subplot, the green line represents the quantity calculated using measured (and variable with time) $(U/Th)_{det}$, the orange line represents the quantity calculated with $(U/Th)_{det} = 0.4$, and the red line represents the variable calculated with $(U/Th)_{det} = 0.8$).

changes in $(U/Th)_{det}$ value (i.e., from 0.4 to 0.8) are responsible for an average age change of 65 years and a maximum age change of about 130 years (Figure 4).

The drastic changes in the $(U/Th)_{det}$ value applied here result in a shift in ages within the uncertainty of the age model (Table S6). In short, for SU90-08, the combined uncertainties of the current marine core dating techniques are larger than the uncertainty resulting from the choice of $(U/Th)_{det}$ value. In the absence of a quantitative evaluation of temporal variations in the $(U/Th)_{det}$ value for the other cores, the effect of the choice of $(U/Th)_{det}$ value on Th normalization based chronologies was tested for constant and variable

$(U/Th)_{det}$ as detailed in Table S12 and Figures S7 and S8. We find that the age model produced by Th normalization is not significantly affected by the choice of the $(U/Th)_{det}$ value for core SU90-03. Core SU81-18 age model is the most affected by changes in the $(U/Th)_{det}$ value, which is consistent with the high terrigenous supply at this location (Missiaen et al., 2018). However, the overall good agreement between the radiocarbon, tie-points, and Th-normalization approaches (Figure 2-Figure S2) gives us confidence in the final age model we produced in this study (see section 4.2; Tables S9 to S11).

4.1.3. Testing the Agreement Between Th Normalization and ^{14}C Dating for the Equatorial Atlantic Core MD03-2705

One approach to evaluate the robustness of the Th-normalization dating method is to compare the sedimentation rate changes inferred from $^{230}Th_{xs,0}$ with the sedimentation rate changes inferred from ^{14}C dates in regions where changes in surface reservoir ages can be considered negligible. We calculated the Th-normalized corrected sedimentation rates for different sets of ^{14}C dates (Figure 5) for core MD03-2705. The sedimentation rate variations based on the calibrated ^{14}C are well reproduced by Th normalization in the upper 100 cm of the core (Figures 5b and 5c). Below 100 cm, the sedimentation rate variations inferred from ^{14}C dates are not reproduced using the Th data (Figures 5d–5f) due to the absence of distinct variability in the $^{230}Th_{xs,0}$ record.

It is unclear whether the dampened variability is real or could be related to changes in lateral sediment redistribution. This might be possible because the focusing factor decreases around 100 cm (Figure 3), where the sedimentation rate change is not reproduced by Th normalization (Figure 5). Another explanation might be that the planktonic foraminifer ^{14}C dates produce artificial sedimentation rate changes. It is indeed well known that a set of radiocarbon dates can create age reversals or artificial sedimentation rate spikes. This could be related to several phenomena, linked to the nature of the archive, such as sediment bioturbation, variations in foraminifer abundances, or changes in chemical erosion (see Mekik, 2014, for a detailed review). Finally, although core MD03-2705 is located in the tropics, and thus is less prone to reservoir age changes than cores located north of 40°N, two processes may have affected its surface reservoir ages and hence the sedimentation rate history reconstructed from the calibrated radiocarbon dates. First, glacial-interglacial changes in atmospheric partial pressure in CO_2 would increase the glacial reservoir ages by a couple hundred of years (Galbraith et al., 2015). Second, the core is located close to the Northwestern African upwelling area, and changes in the upwelling intensity and/or location could have also modified the local reservoir age since the upwelled waters bring ^{14}C-depleted carbon to the surface. However, this latter effect on the reservoir age remains difficult to assess.

Further investigation is required to distinguish which of the hypotheses is the most likely in this case. This could be achieved by measuring additional radiocarbon ages from different foraminifer species and at higher resolution.

4.2. A New Tie-Point for HS1 Cooling?

The age-depth relationships of sediment cores located north of 40°N in the Atlantic rely on the alignment of marine surface temperature records with well-dated Greenland ice temperature records. However, there is a lack of well-defined high amplitude events in the Greenland record that can be used as a tie point between 14.7 and 23.3 ka. Previous research (e.g., McGee et al., 2010; Serno et al., 2015) has shown a correspondence between cold temperatures and increased dust deposition in Greenland, both on glacial-interglacial timescales and also during abrupt climate events. For instance, the onsets of Greenland cold stadials are systematically associated with sharp increases in Greenland dust or dust proxies such as Ca^{2+} (e.g., Ruth et al., 2007; Serno et al., 2015). This synchronicity between temperature and dust changes in the North Atlantic region is indicative of a role of atmospheric circulation in the transitions in and out of the cold stadial conditions. Our revised chronologies for North Atlantic cores SU90-08, SU90-03, and SU81-18 (see Tables S9 to S11) further support this link between North Atlantic marine temperature and Greenland dust records at the onset of Heinrich Stadial 1 (HS1).

The three marine records on the revised chronologies consist of SST reconstructions and the percentage of *N. pachyderma* sinistral (%Nps), a polar foraminifer species, which can serve as a proxy of SST in the North Atlantic (see Eynaud et al., 2009; Govin et al., 2012). For these three cores, the use of Th normalization appears to be a valid approach because (i) there is no evidence for significant focusing variations (see

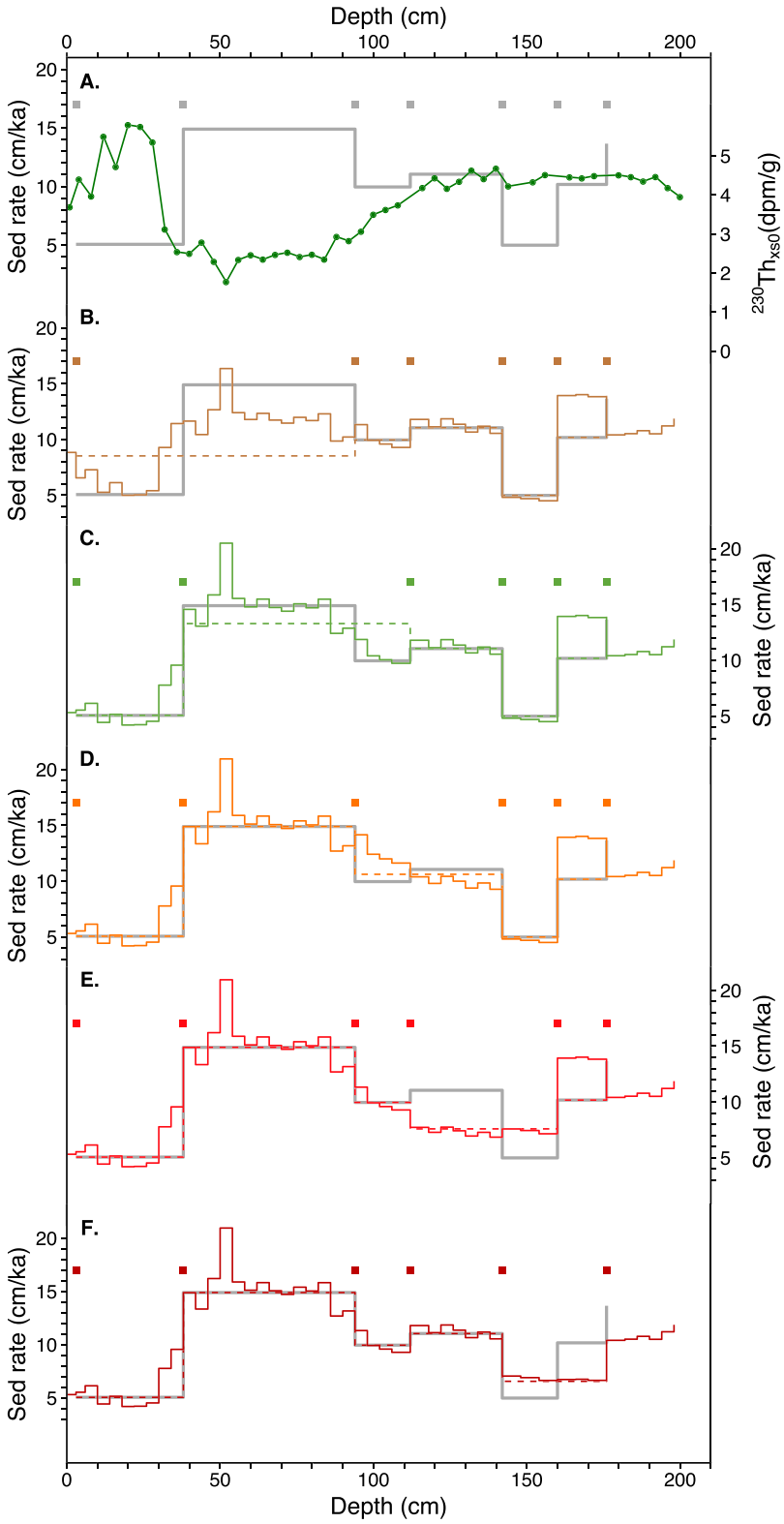

Figure 5. Comparison of sedimentation rate changes inferred from calibrated ^{14}C dates and Th data for MD03-2705. For each subplot, the squares indicate the used ^{14}C dates, the bold grey line represents the initial sedimentation rate obtained from linear interpolation when using all the ^{14}C dates, the dashed colored line represents the initial sedimentation rate obtained from linear interpolation using the considered ^{14}C dates, and the colored line represents the corrected sedimentation rate obtained by Th normalization. On the subplot (a), the green line corresponds to the $^{230}Th_{xs,0}$ data.

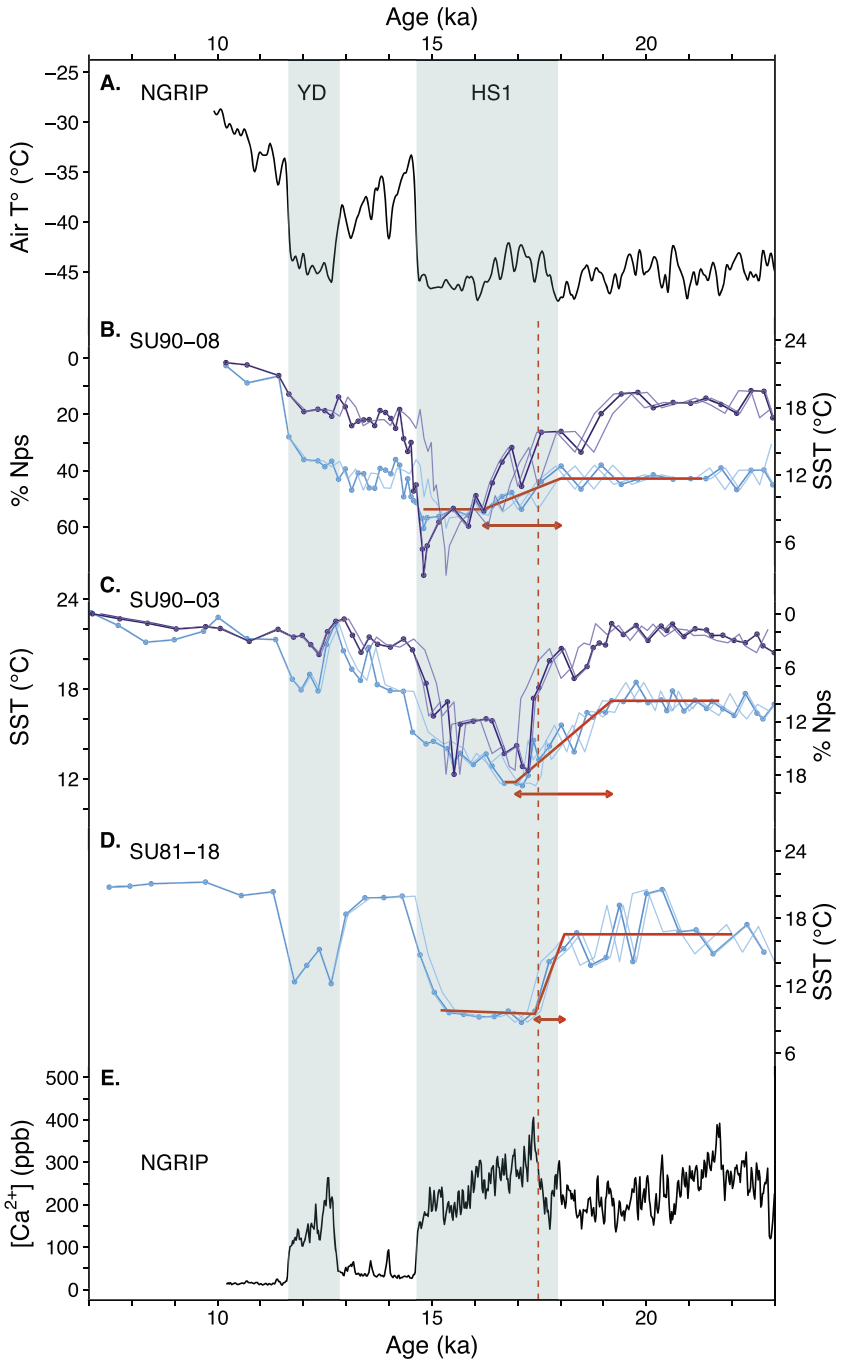

Figure 6. Sea surface temperature (SST) reconstructions for the cores SU90-03, SU90-08, and SU81-18 compared with NGRIP air temperature reconstruction and Ca^{2+} record. (a) NGRIP air temperature reconstruction (Kindler et al., 2014). (b–d) Summer SST reconstructions (light blue) and *%N. pachyderma* s. (Nps; dark blue) data for SU90-08 (b), SU90-03 (d), and SU81-18 (e). (e) NGRIP Ca^{2+} record (Seierstad et al., 2014). The revised chronologies presented here are derived from radiocarbon dates (during the Holocene), SST alignment (for the last deglaciation), and Th normalization (between the above-cited chronological markers). The thin lines represent the envelope curves obtained when moving the SST alignment tie points within the uncertainties described in Tables S6 to S8. Precise beginning and end of the cooling observed at the beginning of HS1 were evaluated for the three records using the Rampfit software (Mudelsee, 2000) and are represented by the bold red line. Bands are as in previous figures. The red vertical dashed line represents the midramp of the increase in NGRIP Ca^{2+} at 17.48 ka.

section 4.1.1) and (ii) changes in $(U/Th)_{det}$ should not affect the produced age models beyond the dating uncertainties (see section 4.1.2). The time period for which Th normalization has the most significant impact is in the poorly constrained interval between 14.7 and 23.3 ka. Indeed, by providing additional stratigraphic information between the SST alignment tie points, the use of Th normalization helps to better constrain the three SST records in this interval. Within the dating uncertainties, we find that the three SST records have considerable consistency in the timing of HS1 cooling (Figure 6). Furthermore, the cooling marking the beginning of HS1 in the three studied North Atlantic SST records is synchronous, within dating uncertainties, with the abrupt increase in Greenland Ca^{2+} that can be interpreted as a major event of dust deposition (Seierstad et al., 2014; Figure 6). The considered sharp increase in NGRIP Ca^{2+} starts at 17.75 ± 0.16 (1σ) and ends at 17.37 ± 0.16 (1σ) ka according to the NGRIP age scale (Andersen et al., 2006; Rasmussen et al., 2006; Wolff et al., 2010).

In detail, we note that the SST transition abruptness varies between our three marine records SU81-18, SU90-08, and SU90-03. The abruptness of a marine SST transition depends on the duration of the cooling but also on the core sample spacing, sedimentation rate, and the bioturbation level. The three studied cores have different average sedimentation rate: <6.5 cm/ka for SU90-08 and SU90-03, whereas SU81-18 has an average sedimentation rate of about 30 cm/ka. Consequently, considering a typical mixed layer of 10 cm, the records from the low sedimentation rate cores SU90-08 and SU90-03 are more affected by bioturbation and likely display smoother transitions (Bard, Arnold, Maurice, et al., 1987). Furthermore, the two types of SST reconstructions (foraminifera assemblages and %Nps) do not show synchronous changes at the onset of HS1: In SU90-03 the foraminifer assemblage SST reconstruction displays a progressive cooling, whereas the %Nps is characterized by a stepwise and more marked SST cooling.

Despite variations of the SST cooling abruptness in our three North Atlantic records, and within the uncertainties, the midpoint of the NGRIP Ca^{2+} record dated at 17.48 ± 0.21 (1σ) ka falls between the onset and end of the SST transition in our three marine records. We thus propose to use the sharp increase in Ca^{2+} dated at 17.48 ka $\pm$ 0.21 ky (1σ) as a new tie point corresponding to the midpoint of SST decreases in the northern North Atlantic sediment cores.

The choice of tying the midpoint of the SST transition is made because (1) it is a robust feature relatively easy to identify and (2) it follows the recommendations from the INTIMATE (Integration of Ice Core, Marine and Terrestrial records of the North Atlantic) for "marine event-based chronostratigraphies in the North Atlantic" (Austin & Hibbert, 2012). Filling the gap between 14.7 and 23.3 ka, this new tie point has the potential to considerably improve North Atlantic marine chronologies based on the alignment of SST to NGRIP.

Based on the arguments above, we can assess what would be the best possible precision of northern North Atlantic core chronologies over the HS1 time interval. To date, it is difficult to robustly evaluate the uncertainty on Th-normalization-based age models since there is no available software for age model construction and uncertainty propagation including Th normalization. To evaluate the chronological uncertainties, we tested the effect of changing the tie-point positions within the uncertainties described in Tables S6 to S8 (Figure 6). The chosen position of the tie point within the defined uncertainties does not change the above conclusions (Figure 6). Furthermore, we can estimate the dating uncertainty of our new tie point to 0.21 ky by quadratic propagation of the uncertainty of the NGRIP GICC05 chronology at 17.48 ka (Wolff et al., 2010) and the duration of the Ca^{2+} transition. The precision of marine core chronologies derived from SST alignment is limited by both the temporal resolution of the SST record and the dating uncertainties of the target tie points. The age models uncertainties associated to the onset of HS1 ranges from about 300 years in the best case (SU81-18) to about 900 years for cores with low sedimentation rate and smooth SST transitions (e.g., SU90-08 and SU90-03; see Figure S9).

5. Conclusions

Th normalization provides a powerful yet underused tool to refine marine core chronologies. However, the successful use of this method requires robust constraints on the underlying assumptions. Among the six major assumptions, two require particular attention: (i) the lateral sediment redistribution should remain broadly constant over the studied climatic period, and (ii) the $(U/Th)_{det}$ temporal variations are sufficiently constrained for locations with significant detrital inputs. Monitoring changes in lateral sediment

redistribution is crucial because untracked changes in the sedimentation regime can artificially dampen or amplify the reconstructed sedimentation rate history, but to date it remains a challenge because of the lack of a direct and independent proxy for focusing factor. To address the first assumption, we evaluated the lateral sediment redistribution variations for our study locations looking at the published magnetic properties and calculating the focusing factor based on $^{230}Th_{xs,0}$. To evaluate the second assumption, we investigated the impact of the choice and temporal variations of the $(U/Th)_{det}$ value on the chronologies built using the Th-normalization technique. Our results show that the age model changes due to variations in the $(U/Th)_{det}$ value are small compared to the uncertainties on the tie points themselves. Finally, we have found good agreement between sedimentation rate changes reconstructed from radiocarbon dates and Th-normalization technique for tropical Atlantic core MD03-2705.

Using combined information from SST alignment tie points, radiocarbon dates, and Th normalization, we established comprehensive and high-resolution sedimentation rate history and chronologies for North Atlantic cores SU90-03, SU90-08, and SU81-18. Our results highlight that Th normalization produces an increase in sedimentation rates across Heinrich events for core SU90-08, as is expected from an increased supply of detrital material from melting icebergs. Interestingly, Th normalization has the most significant impact on SU90-08, SU90-03, and SU81-18 chronologies in the interval between 14.7 and 23.3 ka where no abrupt climate event is recorded in Greenland ice $\delta^{18}O$ or temperature reconstructions. We show that SST records from these three North Atlantic records display great consistency. The timing of SST cooling at the onset of the HS1 appears synchronous with the Greenland Ca^{2+} record, interpreted as a proxy for dust deposition. Thus, we propose the use of this event dated at 17.48 ± 0.21 (1σ) as a new tie point corresponding to the midslope of HS1 cooling in North Atlantic marine SST records. The use of this new tie point could lead to a great advance in North Atlantic age modeling as it fills the gap of tie points between 14.7 and 23.3 ka and allows to better constrain North Atlantic records in this crucial time interval for the study of HS1 and the last deglaciation.

Future work is necessary to further test consistency between radiocarbon-based chronologies and alternative dating methods such as tie-point alignment and Th normalization. If Th normalization becomes more broadly used as a tool to refine sedimentation rate history, including this age information in Bayesian age model software would become necessary to better evaluate the uncertainty propagation taking into account the uncertainties from $^{230}Th_{xs,0}$ calculation. Finally, additional precise and comprehensive North Atlantic chronologies are necessary to test the use of the NGRIP Ca^{2+} 17.48 ka event as a new alignment tie point for constraining North Atlantic sediment age models.

Acknowledgments
This is a contribution to ERC project ACCLIMATE; the research leading to these results has received funding from the European Research Council under the European Union's Seventh Framework Programme (FP7/2007-2013)/ERC grant agreement 339108. S. L. J. acknowledges funding from the Swiss National Science Foundation (grants PBEZ2-111588 and PP00P2_144811). S. P. acknowledges the support from the ENS de Lyon for a CRCT (research sabbatical at the LSCE and MPIC). A. B. and R. G. were funded by NERC grant NE/M004619/1. We thank N. Meckler and B. Malaizé for the information provided about core MD03-2705, R. François for his fruitful comments about the focusing factor, M. Soon for her help during SU90-03 $^{230}Th_{xs,0}$ data acquisition, and S. Moreira for his help with R programming. This is LSCE contribution 6570. Conflict of interests: The authors declare that they have no conflict of interests. Data availability: The data are given as tables in the supporting information and is available online on Pangaea database (https://www.pangaea.de/).

References

Adkins, J. F., Boyle, E. A., Keigwin, L., & Cortijo, E. (1997). Variability of the North Atlantic thermohaline circulation during the last interglacial period. *Nature*, *390*(6656), 154–156. https://doi.org/10.1038/36540

Andersen, K. K., Svensson, A., Johnsen, S. J., Rasmussen, S. O., Bigler, M., Röthlisberger, R., et al. (2006). The Greenland ice core chronology 2005, 15–42 ka. Part 1: constructing the time scale. *Quaternary Science Reviews*, *25*(23-24), 3246–3257. https://doi.org/10.1016/j.quascirev.2006.08.002

Austin, W. E. N., & Hibbert, F. D. (2012). Tracing time in the ocean: A brief review of chronological constraints (60–8 kyr) on North Atlantic marine event-based stratigraphies. *Quaternary Science Reviews*, *36*, 28–37. https://doi.org/10.1016/j.quascirev.2012.01.015

Bacon, M. P., & Rosholt, J. N. (1982). Accumulation rates of Th-230, Pa-231, and some transition metals on the Bermuda Rise. *Geochimica et Cosmochimica Acta*, *46*(4), 651–666. https://doi.org/10.1016/0016-7037(82)90166-1

Bard, E., Arnold, M., Duprat, J., Moyes, J., & Duplessy, J.-C. (1987). Reconstruction of the last deglaciation: Deconvolved records of $\delta^{18}O$ profiles, micropaleontological variations and accelerator mass spectrometric ^{14}C dating. *Climate Dynamics*, *1*(2), 101–112. https://doi.org/10.1007/BF01054479

Bard, E., Arnold, M., Mangerud, J., Paterne, M., Labeyrie, L., Duprat, J., et al. (1994). The North Atlantic atmosphere-sea surface ^{14}C gradient during the Younger Dryas climatic event. *Earth and Planetary Science Letters*, *126*(4), 275–287. https://doi.org/10.1016/0012-821X(94)90112-0

Bard, E., Arnold, M., Maurice, P., Duprat, J., Moyes, J., & Duplessy, J.-C. (1987). Retreat velocity of the North Atlantic polar front during the last deglaciation determined by ^{14}C accelerator mass spectrometry. *Nature*, *328*(6133), 791–794. https://doi.org/10.1038/328791a0

Barker, S., Broecker, W., Clark, E., & Hajdas, I. (2007). Radiocarbon age offsets of foraminifera resulting from differential dissolution and fragmentation within the sedimentary bioturbated zone. *Paleoceanography*, *22*, PA2205. https://doi.org/10.1029/2006PA001354

Blaauw, M. (2010). Methods and code for 'classical' age-modelling of radiocarbon sequences. *Quaternary Geochronology*, *5*(5), 512–518. https://doi.org/10.1016/j.quageo.2010.01.002

Böhm, E., Lippold, J., Gutjahr, M., Frank, M., Blaser, P., Antz, B., et al. (2015). Strong and deep Atlantic meridional overturning circulation during the last glacial cycle. *Nature*, *517*(7532), 73–76. https://doi.org/10.1038/nature14059

Bondevik, S., Mangerud, J., Birks, H. H., Gulliksen, S., & Reimer, P. (2006). Changes in North Atlantic radiocarbon reservoir ages during the Allerød and Younger Dryas. *Science*, *312*(5779), 1514–1517. https://doi.org/10.1126/science.1123300

Bourne, M. D., Mac Niocaill, C., Thomas, A. L., Knudsen, M. F., & Henderson, G. M. (2012). Rapid directional changes associated with a 6.5 kyr-long Blake geomagnetic excursion at the Blake–Bahama Outer Ridge. *Earth and Planetary Science Letters*, *333-334*, 21–34. https://doi.org/10.1016/j.epsl.2012.04.017

Bourne, M. D., Thomas, A. L., Mac Niocaill, C., & Henderson, G. M. (2012). Improved determination of marine sedimentation rates using $^{230}Th_{xs}$. *Geochemistry, Geophysics, Geosystems*, *13*, Q09017. https://doi.org/10.1029/2012GC004295

Broecker, W. (2008). Excess sediment ^{230}Th: Transport along the sea floor or enhanced water column scavenging? *Global Biogeochemical Cycles*, *22*, GB1006. https://doi.org/10.1029/2007GB003057

Broecker, W., Barker, S., Clark, E., Hajdas, I., & Bonani, G. (2006). Anomalous radiocarbon ages for foraminifera shells. *Paleoceanography*, *21*, PA2008. https://doi.org/10.1029/2005PA001212

Chapman, M. R., Shackleton, N. J., & Duplessy, J.-C. (2000). Sea surface temperature variability during the last glacial–interglacial cycle: Assessing the magnitude and pattern of climate change in the North Atlantic. *Palaeogeography, Palaeoclimatology, Palaeoecology*, *157*(1-2), 1–25. https://doi.org/10.1016/S0031-0182(99)00168-6

Chase, Z., Anderson, R. F., Fleisher, M. Q., & Kubik, P. W. (2002). The influence of particle composition and particle flux on scavenging of Th, Pa and Be in the ocean. *Earth and Planetary Science Letters*, *204*(1-2), 215–229. https://doi.org/10.1016/S0012-821X(02)00984-6

Choi, M. S., Francois, R., Sims, K., Bacon, M. P., Brown-Leger, S., Fleer, A. P., et al. (2001). Rapid determination of ^{230}Th and ^{231}Pa in seawater by desolvated micro-nebulization inductively coupled plasma magnetic sector mass spectrometry. *Marine Chemistry*, *76*(1-2), 99–112. https://doi.org/10.1016/S0304-4203(01)00050-0

Clement, A. C., & Peterson, L. C. (2008). Mechanisms of abrupt climate change of the last glacial period. *Reviews of Geophysics*, *46*, RG4002. https://doi.org/10.1029/2006RG000204

Cortijo, E., Lehman, S., Keigwin, L., Chapman, M., Paillard, D., & Labeyrie, L. (1999). Changes in meridional temperature and salinity gradients in the North Atlantic Ocean (30°–72°N) during the last interglacial period. *Paleoceanography*, *14*(1), 23–33. https://doi.org/10.1029/1998PA900004

Costa, K., & McManus, J. (2017). Efficacy of ^{230}Th normalization in sediments from the Juan de Fuca Ridge, northeast Pacific Ocean. *Geochimica et Cosmochimica Acta*, *197*, 215–225. https://doi.org/10.1016/j.gca.2016.10.034

Eynaud, F., de Abreu, L., Voelker, A., Schönfeld, J., Salgueiro, E., Turon, J.-L., et al. (2009). Position of the Polar Front along the western Iberian margin during key cold episodes of the last 45 ka. *Geochemistry, Geophysics, Geosystems*, *10*, Q07U05. https://doi.org/10.1029/2009GC002398

François, R. (2007). Paleoflux and paleocirculation from sediment 230Th and 231Pa/230Th. In *Proxies in Late Cenozoic paleoceanography* (pp. 681–716). Amsterdam: Elsevier.

François, R., Frank, M., Rutgers van der Loeff, M. M., & Bacon, M. P. (2004). ^{230}Th normalization: An essential tool for interpreting sedimentary fluxes during the Late Quaternary. *Paleoceanography*, *19*, PA1018. https://doi.org/10.1029/2003PA000939

Froelich, P. N., Malone, P. N., Hodell, D. A., Ciesielski, P. F., Warnke, D. A., Westall, F., et al. (1991). Biogenic opal and carbonate accumulation rates in the subantarctic South Atlantic: The late Neogene of Meteor Rise Site 704. In *Proceedings of the Ocean Drilling Program*, Scientific Results (Vol. *114*, pp. 515–550). College Station, TX: Ocean Drilling Program.

Galbraith, E. D., Kwon, E. Y., Bianchi, D., Hain, M. P., & Sarmiento, J. L. (2015). The impact of atmospheric pCO_2 on carbon isotope ratios of the atmosphere and ocean. *Global Biogeochemical Cycles*, *29*, 307–324. https://doi.org/10.1002/2014GB004929

Gherardi, J.-M., Labeyrie, L., McManus, J. F., Francois, R., Skinner, L. C., & Cortijo, E. (2005). Evidence from the Northeastern Atlantic basin for variability in the rate of the meridional overturning circulation through the last deglaciation. *Earth and Planetary Science Letters*, *240*(3-4), 710–723. https://doi.org/10.1016/j.epsl.2005.09.061

Gherardi, J.-M., Labeyrie, L., Nave, S., Francois, R., McManus, J. F., & Cortijo, E. (2009). Glacial-interglacial circulation changes inferred from ^{231}Pa/^{230}Th sedimentary record in the North Atlantic region. *Paleoceanography*, *24*, PA2204. https://doi.org/10.1029/2008PA001696

Govin, A., Braconnot, P., Capron, E., Cortijo, E., Duplessy, J.-C., Jansen, E., et al. (2012). Persistent influence of ice sheet melting on high northern latitude climate during the early Last Interglacial. *Climate of the Past*, *8*(2), 483–507. https://doi.org/10.5194/cp-8-483-2012

Hall, I. R., Evans, H. K., & Thornalley, D. J. R. (2011). Deep water flow speed and surface ocean changes in the subtropical North Atlantic during the last deglaciation. *Global and Planetary Change*, *79*(3-4), 255–263. https://doi.org/10.1016/j.gloplacha.2010.12.001

Henderson, G. M., & Anderson, R. F. (2003). The U-series toolbox for paleoceanography. *Reviews in Mineralogy and Geochemistry*, *52*(1), 493–531. https://doi.org/10.2113/0520493

Henderson, G. M., Heinze, C., Anderson, R. F., & Winguth, A. M. (1999). Global distribution of the ^{230}Th flux to ocean sediments constrained by GCM modelling. *Deep Sea Research Part I: Oceanographic Research Papers*, *46*(11), 1861–1893. https://doi.org/10.1016/S0967-0637(99)00030-8

Henry, L. G., McManus, J. F., Curry, W. B., Roberts, N. L., Piotrowski, A. M., & Keigwin, L. D. (2016). North Atlantic ocean circulation and abrupt climate change during the last glaciation. *Science*, *353*(6298), 470–474. https://doi.org/10.1126/science.aaf5529

Jacobel, A. W., McManus, J. F., Anderson, R. F., & Winckler, G. (2017). Climate-related response of dust flux to the central equatorial Pacific over the past 150 kyr. *Earth and Planetary Science Letters*, *457*, 160–172. https://doi.org/10.1016/j.epsl.2016.09.042

Jullien, E., Grousset, F., Malaizé, B., Duprat, J., Sanchez-Goni, M. F., Eynaud, F., et al. (2007). Low-latitude "dusty events" vs. high-latitude "icy Heinrich events". *Quaternary Research*, *68*(3), 379–386. https://doi.org/10.1016/j.yqres.2007.07.007

Key, R. M., Kozyr, A., Sabine, C. L., Lee, K., Wanninkhof, R., Bullister, J. L., et al. (2004). A global ocean carbon climatology: Results from Global Data Analysis Project (GLODAP). *Global Biogeochemical Cycles*, *18*, GB4031. https://doi.org/10.1029/2004GB002247

Kienast, S. S., Kienast, M., Mix, A. C., Calvert, S. E., & François, R. (2007). Thorium-230 normalized particle flux and sediment focusing in the Panama Basin region during the last 30,000 years. *Paleoceanography*, *22*, PA2213. https://doi.org/10.1029/2006PA001357

Kindler, P., Guillevic, M., Baumgartner, M., Schwander, J., Landais, A., & Leuenberger, M. (2014). Temperature reconstruction from 10 to 120 kyr b2k from the NGRIP ice core. *Climate of the Past*, *10*(2), 887–902. https://doi.org/10.5194/cp-10-887-2014

Kissel, C. (2005). Magnetic signature of rapid climatic variations in glacial North Atlantic: A review. *Comptes Rendus Geoscience*, *337*(10-11), 908–918. https://doi.org/10.1016/j.crte.2005.04.009

Lougheed, B. C., & Obrochta, S. P. (2019). A Rapid, Deterministic age-depth modeling routine for geological sequences with inherent depth uncertainty. *Paleoceanography*, *34*, 122–133. https://doi.org/10.1029/2018PA003457

Lynch-Stieglitz, J. (2017). The Atlantic meridional overturning circulation and abrupt climate change. *Annual Review of Marine Science*, *9*(1), 83–104. https://doi.org/10.1146/annurev-marine-010816-060415

Marcantonio, F., Anderson, R. F., Higgins, S., Stute, M., Schlosser, P., & Kubik, P. (2001). Sediment focusing in the central equatorial Pacific Ocean. *Paleoceanography*, *16*(3), 260–267. https://doi.org/10.1029/2000PA000540

Marcantonio, F., Lyle, M., & Ibrahim, R. (2014). Particle sorting during sediment redistribution processes and the effect on ^{230}Th-normalized mass accumulation rates. *Geophysical Research Letters*, *41*, 5547–5554. https://doi.org/10.1002/2014GL060477

Matsuzaki, K. M. R., Eynaud, F., Malaizé, B., Grousset, F. E., Tisserand, A., Rossignol, L., et al. (2011). Paleoceanography of the Mauritanian margin during the last two climatic cycles: From planktonic foraminifera to African climate dynamics. *Marine Micropaleontology*, *79*(3-4), 67–79. https://doi.org/10.1016/j.marmicro.2011.01.004

McGee, D., Broecker, W. S., & Winckler, G. (2010). Gustiness: The driver of glacial dustiness? *Quaternary Science Reviews*, *29*(17-18), 2340–2350. https://doi.org/10.1016/j.quascirev.2010.06.009

Meckler, A. N., Sigman, D. M., Gibson, K. A., François, R., Martínez-García, A., Jaccard, S. L., et al. (2013). Deglacial pulses of deep-ocean silicate into the subtropical North Atlantic Ocean. *Nature*, *495*(7442), 495–498. https://doi.org/10.1038/nature12006

Mekik, F. (2014). Radiocarbon dating of planktonic foraminifer shells: A cautionary tale. *Paleoceanography*, *29*, 13–29. https://doi.org/10.1002/2013PA002532

Missiaen, L., Pichat, S., Waelbroeck, C., Douville, E., Bordier, L., Dapoigny, A., et al. (2018). Downcore Variations of Sedimentary Detrital (^{238}U/^{232}Th) Ratio: Implications on the Use of $^{230}Th_{xs}$ and $^{231}Pa_{xs}$ to reconstruct sediment flux and ocean circulation. *Geochemistry, Geophysics, Geosystems*, *19*, 2560–2573. https://doi.org/10.1029/2017GC007410

Mudelsee, M. (2000). Ramp function regression: A tool for quantifying climate transitions. *Computers & Geosciences*, *26*(3), 293–307. https://doi.org/10.1016/S0098-3004(99)00141-7

Paillard, D., Labeyrie, L., & Yiou, P. (1996). Macintosh program performs time-series analysis. *Eos, Transactions American Geophysical Union*, *77*(39), 379–379. https://doi.org/10.1029/96EO00259

Parnell, A. C., Haslett, J., Allen, J. R. M., Buck, C. E., & Huntley, B. (2008). A flexible approach to assessing synchroneity of past events using Bayesian reconstructions of sedimentation history. *Quaternary Science Reviews*, *27*(19-20), 1872–1885. https://doi.org/10.1016/j.quascirev.2008.07.009

Rahmstorf, S. (2002). Ocean circulation and climate during the past 120,000 years. *Nature*, *419*(6903), 207–214. https://doi.org/10.1038/nature01090

Ramsey, C. B. (2009). Bayesian analysis of radiocarbon dates. *Radiocarbon*, *51*(1), 337–360. https://doi.org/10.1017/S0033822200033865

Rasmussen, S. O., Andersen, K. K., Svensson, A. M., Steffensen, J. P., Vinther, B. M., Clausen, H. B., et al. (2006). A new Greenland ice core chronology for the last glacial termination. *Journal of Geophysical Research*, *111*, D06102. https://doi.org/10.1029/2005JD006079

Reimer, P. J., Bard, E., Bayliss, A., Beck, J. W., Blackwell, P. G., Ramsey, C. B., et al. (2013). IntCal13 and Marine13 radiocarbon age calibration curves 0–50,000 years cal BP. *Radiocarbon*, *55*(4), 1869–1887. https://doi.org/10.2458/azu_js_rc.55.16947

Robinson, L. F., Henderson, G. M., Hall, L., & Matthews, I. (2004). Climatic control of riverine and seawater uranium-isotope ratios. *Science*, *305*(5685), 851–854. https://doi.org/10.1126/science.1099673

Ruth, U., Bigler, M., Röthlisberger, R., Siggaard-Andersen, M.-L., Kipfstuhl, S., Goto-Azuma, K., et al. (2007). Ice core evidence for a very tight link between North Atlantic and east Asian glacial climate. *Geophysical Research Letters*, *34*, L03706. https://doi.org/10.1029/2006GL027876

Seierstad, I. K., Abbott, P. M., Bigler, M., Blunier, T., Bourne, A. J., Brook, E., et al. (2014). Consistently dated records from the Greenland GRIP, GISP2 and NGRIP ice cores for the past 104 ka reveal regional millennial-scale δ^{18}O gradients with possible Heinrich event imprint. *Quaternary Science Reviews*, *106*, 29–46. https://doi.org/10.1016/j.quascirev.2014.10.032

Serno, S., Winckler, G., Anderson, R. F., Maier, E., Ren, H., Gersonde, R., & Haug, G. H. (2015). Comparing dust flux records from the Subarctic North Pacific and Greenland: Implications for atmospheric transport to Greenland and for the application of dust as a chronostratigraphic tool. *Paleoceanography*, *30*, 583–600. https://doi.org/10.1002/2014PA002748

Suman, D. O., & Bacon, M. P. (1989). Variations in Holocene sedimentation in the North American Basin determined from ^{230}Th measurements. *Deep Sea Research Part A. Oceanographic Research Papers*, *36*(6), 869–878. https://doi.org/10.1016/0198-0149(89)90033-2

Svensson, A., Andersen, K. K., Bigler, M., Clausen, H. B., Dahl-Jensen, D., Davies, S. M., et al. (2006). The Greenland ice core chronology 2005, 15–42ka. Part 2: Comparison to other records. *Quaternary Science Reviews*, *25*(23-24), 3258–3267. https://doi.org/10.1016/j.quascirev.2006.08.003

Thornalley, D. J. R., Barker, S., Broecker, W. S., Elderfield, H., & McCave, I. N. (2011). The deglacial evolution of North Atlantic Deep Convection. *Science*, *331*(6014), 202–205. https://doi.org/10.1126/science.1196812

Vidal, L., Labeyrie, L., Cortijo, E., Arnold, M., Duplessy, J. C., Michel, E., et al. (1997). Evidence for changes in the North Atlantic Deep Water linked to meltwater surges during the Heinrich events. *Earth and Planetary Science Letters*, *146*(1-2), 13–27. https://doi.org/10.1016/S0012-821X(96)00192-6

Vinther, B. M., Clausen, H. B., Johnsen, S. J., Rasmussen, S. O., Andersen, K. K., Buchardt, S. L., et al. (2006). A synchronized dating of three Greenland ice cores throughout the Holocene. *Journal of Geophysical Research*, *111*, D13102. https://doi.org/10.1029/2005JD006921

Waelbroeck, C., Duplessy, J.-C., Michel, E., Labeyrie, L., Paillard, D., & Duprat, J. (2001). The timing of the last deglaciation in North Atlantic climate records. *Nature*, *412*(6848), 724–727. https://doi.org/10.1038/35089060

Wolff, E. W., Chappellaz, J., Blunier, T., Rasmussen, S. O., & Svensson, A. (2010). Millennial-scale variability during the last glacial: The ice core record. *Quaternary Science Reviews*, *29*(21-22), 2828–2838. https://doi.org/10.1016/j.quascirev.2009.10.013

Wycech, J., Kelly, D. C., & Marcott, S. (2016). Effects of seafloor diagenesis on planktic foraminiferal radiocarbon ages. *Geology*, *44*(7), 551–554. https://doi.org/10.1130/G37864.1

Yu, E.-F., Francois, R., Bacon, M. P., & Fleer, A. P. (2001). Fluxes of ^{230}Th and ^{231}Pa to the deep sea: Implications for the interpretation of excess ^{230}Th and ^{231}Pa/^{230}Th profiles in sediments. *Earth and Planetary Science Letters*, *191*(3-4), 219–230. https://doi.org/10.1016/S0012-821X(01)00410-1